



HAL
open science

Artificial duplication of polarization fatigue in $\text{Pb}(\text{Zr}_{0.54}\text{Ti}_{0.46})\text{O}_3$ thin film capacitors

Rachid Bouregba, Nossikpendou Sama, Caroline Soyer, Gilles Poullain, Denis Remiens

► **To cite this version:**

Rachid Bouregba, Nossikpendou Sama, Caroline Soyer, Gilles Poullain, Denis Remiens. Artificial duplication of polarization fatigue in $\text{Pb}(\text{Zr}_{0.54}\text{Ti}_{0.46})\text{O}_3$ thin film capacitors. *Thin Solid Films*, 2013, 527, pp.327-333. 10.1016/j.tsf.2012.11.098 . hal-00796456

HAL Id: hal-00796456

<https://hal.science/hal-00796456v1>

Submitted on 21 Oct 2021

HAL is a multi-disciplinary open access archive for the deposit and dissemination of scientific research documents, whether they are published or not. The documents may come from teaching and research institutions in France or abroad, or from public or private research centers.

L'archive ouverte pluridisciplinaire **HAL**, est destinée au dépôt et à la diffusion de documents scientifiques de niveau recherche, publiés ou non, émanant des établissements d'enseignement et de recherche français ou étrangers, des laboratoires publics ou privés.



Distributed under a Creative Commons Attribution 4.0 International License

Artificial duplication of polarization fatigue in $\text{Pb}(\text{Zr}_{0.54}\text{Ti}_{0.46})\text{O}_3$ thin film capacitors

Rachid Bouregba^{a,b,c,*}, Nossikpendou Sama^d, Caroline Soyer^d, Gilles Poullain^{a,b,c}, Denis Remiens^d

^a Université de Caen Basse-Normandie, UMR 6508 CRISMAT, F-14032 Caen, France

^b ENSICAEN, UMR 6508 CRISMAT, F-14050 Caen, France

^c CNRS, UMR 6508 CRISMAT, F-14050 Caen, France

^d IEMN-DOAE, CNRS UMR 8520, 59655 Villeneuve d'Ascq Cedex, France

Polarization fatigue in ferroelectric perovskite oxides is a commonly known phenomenon. However no model has promoted consensual interpretation regarding its nature. In this article, the polarization loop of a $\text{Pb}(\text{Zr}_{0.54}\text{Ti}_{0.46})\text{O}_3$ thin film capacitor measured at a given moment of the fatigue process is entirely duplicated after bringing in series with a fresh sample an electrical circuit calibrated in a way to model the aging mechanism. The latter was analyzed by considering time dependent interface properties but invariant bulk values. Unequivocal demonstration is made that fatigue polarization in the studied sample resulted from decline of the electric properties of the interfaces, leading to a decrease in the electric field actually applied to the switching domains. Injection of charge at interface defects, caused by polarization reversal, was probably the vector of these degradations.

1. Introduction

Advent of ferroelectric oxides with the perovskite structure has generated a growing interest for many technological applications, especially for applications as non volatile memories due to large and reversible spontaneous polarization [1]. Unfortunately, ferroelectric capacitors (FECAP) based on this class of materials, like $\text{Pb}(\text{Zr}_x\text{Ti}_{1-x})\text{O}_3$ (PZT) solid solution, suffer from a progressive loss of polarization under application of a long standing repetitive voltage [2]. This reliability issue, recognized as polarization fatigue and especially pronounced when metallic electrodes like platinum are utilized, raised with acuity the question of mass-marketing of silicon integrated thin film memories based on perovskite ferroelectric materials. Beyond the technological barrier which may be overcome by utilizing conducting oxides electrodes [3–9], the fatigue polarization raises also the crucial question of its origin which up to now is enigmatic despite the considerable number of articles devoted to this problem for many decades (see the review articles by A.K. Tagantsev et al. [10] and by X.J. Lou [11]). Examination of the literature data indeed reveals how controversial a matter the fatigue phenomenon is.

In this article, the fatigue stage of a PZT thin film capacitor prepared with platinum electrodes is artificially and entirely duplicated by adding an electrical network in series with a fresh sample. This

circuit is calibrated by assuming that aging is caused by deterioration of the dielectric and electrostatic properties of the interfaces. But this original approach also considers the screening effects of the charge accumulated at the interfaces in the course of aging, as well as the non-linear character of the switching charge. The method failed otherwise.

2. Hysteresis and fatigue measurements – Preliminary analysis

Fig. 1.a) shows the hysteresis loops measured on a 400 nm thick $\text{Pb}(\text{Zr}_{0.54}\text{Ti}_{0.46})\text{O}_3$ capacitor, before and after fatigue cycling. The PZT film was sputtered on $\text{Pt}/\text{TiO}_2/\text{SiO}_2/\text{Si}$ substrate. Platinum was used as the top electrode with a surface area of $1.8 \times 10^{-4} \text{ cm}^2$ defined by photolithography. Details about preparation and structural properties may be found in Ref. [12]. Hysteresis measurements were performed in the virtual ground mode using Radiant Technology and AixACCT measurement systems.

Tilt of the polarization loop accompanied by a drop of the remnant polarization and increase of the coercive fields (E_c) are observed. These hysteresis deformations are typical of fatigue in PZT capacitors although a decrease of coercive field can also be observed [9,13–16]. The basic idea we consider herein refers to previous work in which polarization fatigue in PZT capacitors was proposed to result from the progressive degradation of the dielectric and electrostatic properties of the interfaces, i.e. decrease of interface capacitance and accumulation of charge at the interfaces in the course of aging [17]. The aging mechanism was ascribed to the presence of interface defects

* Corresponding author at: ENSICAEN, UMR 6508 CRISMAT, F-14050 Caen, France. Tel.: +33 2 31 45 13 76; fax: +33 2 31 95 16 00.

E-mail address: rachid.bouregba@ensicaen.fr (R. Bouregba).

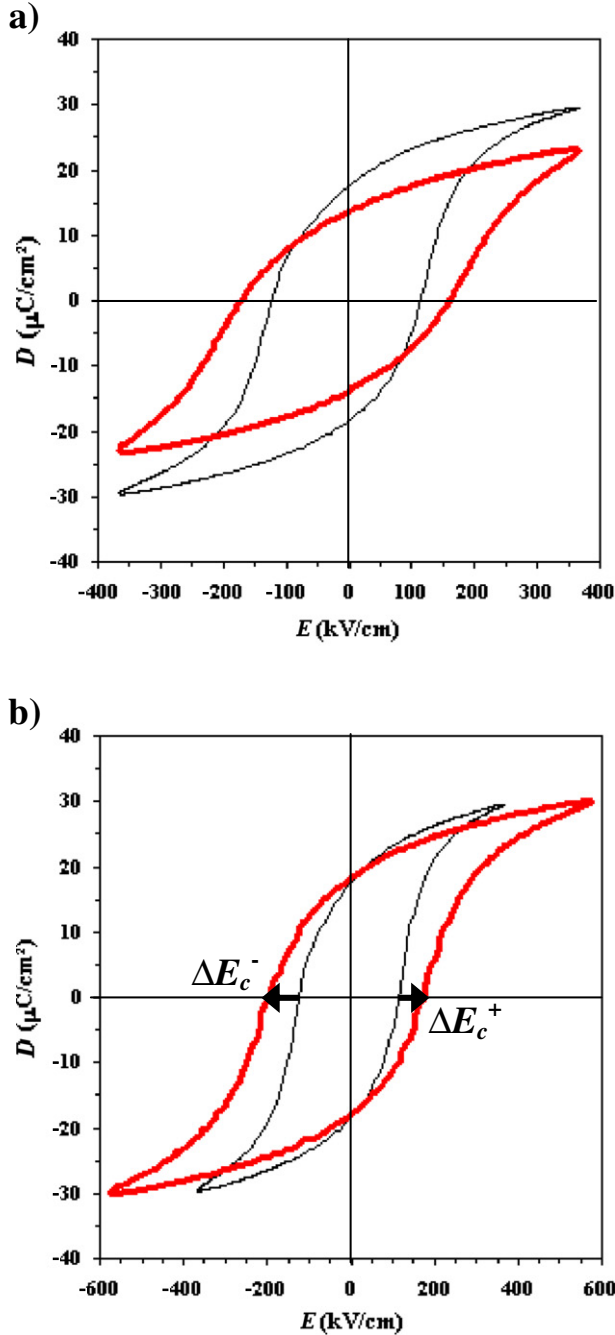


Fig. 1. a) Hysteresis loops of 400 nm thick PZT capacitor before fatigue (thin black line) and after fatigue (thick red line). The measurement frequency was 100 Hz. The fatigue signal was a bipolar square voltage with an amplitude of 2.5 times the coercive voltage and a frequency of 10 kHz. The fatigued loop was plotted after 10^9 cycles. b) Same plot but here the voltage applied to the fatigued capacitor was set in order to achieve the same maximum electric displacement than in a). ΔE_c^+ and ΔE_c^- represent the increase of coercive fields obtained under these conditions.

with large time constant [17,18]. This is summarized in Fig. 2 which depicts the conditions before and after fatigue cycling (hereafter labeled as “bf” and “af”, respectively) for a given applied voltage. C_{ibf} , V_{bibf} , C_{iaf} and V_{biaf} are the interface capacitances and the interface built-in potentials at these two moments. For convenience of the analysis, the effects of both interfaces are included in only one. Note that the ferroelectric capacitor, of thickness d , is assumed to contain damaged interfaces from the virgin stage, as previously established to explain the thickness dependence of the dielectric and ferroelectric

properties of PZT films [19,20]. An interface depolarizing field was indeed found to be the common denominator between size effect and fatigue. ϵ_f is the permittivity of the bulk ferroelectric layer and $P_f(E_f)$ the polarization loop due to the switching domains. In the following analysis we will assume that the bulk values, i.e. ϵ_f and the causal relationship between P_f and E_f , remain invariant with fatigue cycling. However the polarization P_f in the bulk layer can fall as a result of a decrease of the electric field E_f applied to it. This event is likely to occur if the interface capacitance declines in the course of aging. D is the electric displacement measured on the plates of the capacitor and E the applied field given by V_{appl}/d .

The impact of aging upon interface potential growth may be accurately evaluated by considering the change in E_c values after taking care that the hysteresis loops before and after fatigue exhibit the same maximum electric displacement (D_{max}) [17]. This condition, achieved by adjusting the voltage applied to the fatigued sample, compensates for the voltage drop across the interface capacitance and makes it possible to set the polarization in the bulk ferroelectric layer at the same value as before fatigue cycling (see Fig. 1.b)).

We first focus on the dielectric properties of the interfaces. The electrostatic effects, i.e. those related to interface potential, will be assessed later on.

If deterioration of the interface dielectric properties actually occurs in the film after fatigue cycling, then we can define ΔC_i such that:

$$\frac{1}{\Delta C_i} = \frac{1}{C_{iaf}} - \frac{1}{C_{ibf}}, \quad (1)$$

where ΔC_i represents the capacitance that should be connected in series with the fresh sample to duplicate the decline of the interface capacitance from C_{ibf} value to C_{iaf} one. Estimation of C_{ibf} and C_{iaf} is possible by utilizing samples with different thicknesses [21,22]. However, the methods usually proposed in the literature for the determination of the interface capacitance are based on small signal impedance measurements; hence, they do not include the non linearity of the system. In the present study, we focus on hysteresis measurements that imply large signal analysis. So to take into account the non-linear (nl) character of the switching charge, we can also define ΔC_i as:

$$\frac{1}{\Delta C_i} = \frac{1}{C_{nlaf}} - \frac{1}{C_{nlbf}}, \quad (2)$$

where C_{nlbf} and C_{nlaf} represent the overall large signal capacitances exhibited by the ferroelectric capacitor before and after fatigue, respectively. With this definition, there is no more need to determine C_{ibf} and C_{iaf} . C_{nlbf} and C_{nlaf} may be estimated as follows:

$$C_{nlbf} = \frac{A \cdot D_{bfRMS}}{V_{applbfRMS}}, \quad \text{and} \quad C_{nlaf} = \frac{A \cdot D_{afRMS}}{V_{applafRMS}} \quad (3)$$

where D_{bfRMS} and D_{afRMS} represent the root mean square (RMS) values of the large signal electric displacement measured along one period of the applied voltage. $V_{applbfRMS}$ and $V_{applafRMS}$ are the RMS values of the applied voltage (a sine wave with a frequency of 100 Hz in this work). A is the area of the ferroelectric capacitor. D_{bfRMS} and D_{afRMS} were calculated from the $D(E)$ loops in Fig. 1.b) by using a numerical integration algorithm. We found $C_{nlbf} = 0.39$ nF and $C_{nlaf} = 0.25$ nF from which we calculate $\Delta C_i = 0.7$ nF. A capacitor of 0.68 nF, the nearest standardized value, was then connected in series with a fresh PZT capacitor. The measured hysteresis loop is displayed in Fig. 3 where the applied voltage was adjusted to obtain the same D_{max} value, as before fatigue. Compared with the actually fatigued sample an excessive voltage was necessary, which means that ΔC_i was underestimated. Moreover much lower E_c are obtained, almost equal to those displayed by the fresh film. Last, remnant values much lower than expected are obtained.

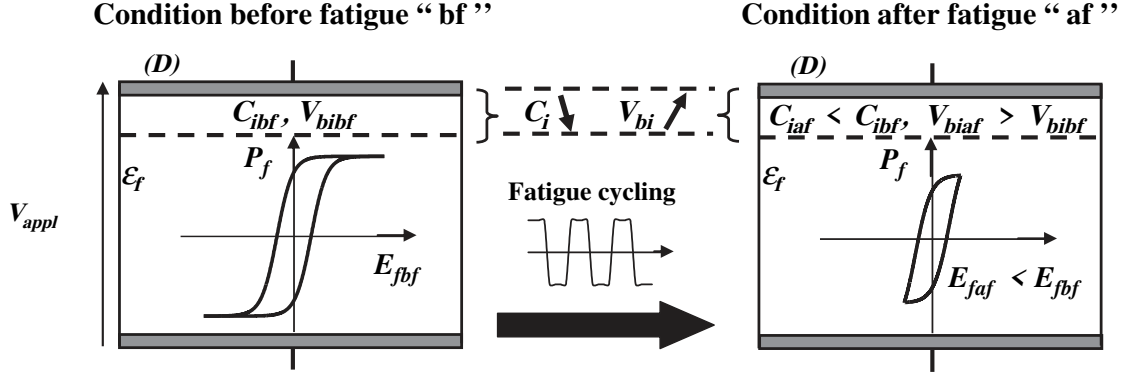


Fig. 2. The PZT thin film capacitor is depicted as a bulk ferroelectric layer exhibiting a polarization loop due to the switching domains. The interface defects are represented as ultra thin charged non ferroelectric layer. Application of a repetitive long-standing stress voltage is assumed to cause a decrease of the interface capacitance and a growth of the interface potential barrier following accumulation of charge.

The mistake in the estimation of ΔC_i stems from the fact that the values of D_{bfRMS} and D_{afRMS} were directly calculated from the contour line of the measured hysteresis loops whereas the latter include deformations caused by the static charge progressively trapped at the interfaces in the course of aging. Only the dynamic part of the charge, showing instantaneous variation with the applied voltage, contributes to the capacitance of the system. Actually, relations (2) and (3) are directly usable with samples showing negligible accumulation of charge. Concerning the observed differences in the E_c and remnant values as discussed above, interface passive layers cannot explain increase in E_c , unless space charge is considered [8,23,24]. Moreover increase in the remnant values (D_r) is also expected because the interface charge is likely to screen the interface depolarizing field [17,20]. Correlatively the series connection with the fresh sample of a relaxed, i.e. not charged, capacitor (Fig. 3) cannot be relevant to duplicate the expected effects of interface space charge, so that duplication of the fatigue stage requires a more sophisticated circuit. Moreover the calibration of ΔC_i needs a detailed modeling including the

non-linear character of the switching charge and the screening effects of the interface charge.

3. Original approach including the non linearities of the switching charge and the screening effects of the accumulated interface charge

The screening effects of the interface static charge can be considered by extracting the inner $P_f(E_f)$ polarization loop from the external $D(E)$ loops measured before and after fatigue cycling. This operation may be carried out by using the following expressions, as already established in previous works [17,19,25]:

$$E_f = \frac{C_i}{C_i + C_f} \left[E - \frac{1}{d} \left(V_{bi} + \frac{A \cdot P_f}{C_i} \right) \right], \quad (4)$$

$$P_f = \left[D - \frac{d}{A} \frac{C_f \cdot C_i}{(C_i + C_f)} \left(E - \frac{V_{bi}}{d} \right) \right] \frac{C_i + C_f}{C_i}, \quad (5)$$

where:

$$C_f = \frac{\epsilon_0 \cdot \epsilon_f \cdot A}{d} \quad \text{and} \quad V_{bi} = \frac{\rho_i d_i^2}{2\epsilon_0 \epsilon_i}. \quad (6)$$

ϵ_0 is the permittivity of free space, ρ_i the interface charge per unit volume, ϵ_i and d_i are the dielectric constant and the thickness of the interface layer, respectively. C_f is the large signal capacitance of the bulk ferroelectric layer whose thickness was made equal to the total thickness d since the interface layers are assumed to be much thinner than the PZT film. The other parameters have already been defined. The subscripts "bf" and "af" have to be added to V_{bi} and C_i depending on whether one considers the virgin or the fatigued stage, respectively. A last point to be outlined before we proceed is the fact that the exact calculation of the $P_f(E_f)$ loop from the $D(E)$ one, requires the sign of V_{bi} in Eqs. (4), (5) and (6) to be changed during one period of the applied voltage according to the following sequence (see Ref. [19] for details and justifications):

$$V_{bi} > 0 \quad \text{when} \quad \frac{\partial V_{appl}}{\partial t} > 0, \quad \text{and} \quad V_{bi} < 0 \quad \text{when} \quad \frac{\partial V_{appl}}{\partial t} < 0.$$

Quantization of the decline of the dielectric and electrostatic properties of the interfaces is now possible owing to an original comparative method between the virgin and the fatigued stage. The topology of the electrical circuit capable of duplicating this deterioration as well as the sign changing of V_{bi} aforementioned will also be proposed. We emphasize that with the original approach outlined below, not

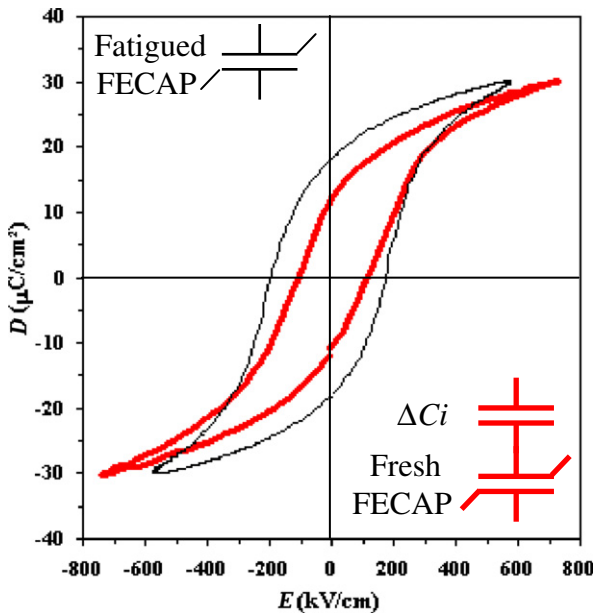


Fig. 3. Hysteresis loops measured on the fatigued PZT capacitor (thin black line) and after connecting a capacitor of 0.68 nF in series with a fresh PZT capacitor (thick red line).

only the screening effects of the interface charge are taken into account, but also the non-linear character of the switching charge because the process is based on large signal hysteresis measurements.

3.1. Determination of ΔC_i and of the growth of the interface potential barrier ΔV_{bi}

Since the properties of the bulk ferroelectric layer are not diminished by fatigue cycling, the $P_f(E_f)$ loop can be computed from the $D(E)$ loop measured on the fresh sample rather than on the fatigued one. As we are only concerned with the *changes* in the interface values caused by fatigue, i.e. ΔV_{bi} and ΔC_i , where $\Delta V_{bi} = V_{biaf} - V_{bibf}$ represents the growth of the potential barrier due to accumulation of interface charge, then the knowledge of C_{ibf} and V_{bibf} at the virgin stage is unnecessary. These values will therefore be disregarded by arbitrarily considering C_{ibf} infinite and V_{bibf} null in the relations (4) and (5). This assumes perfect interfaces even though actually the latter are damaged [19,20]. There is no contradiction in doing so because in that case we do not calculate the actual polarization loop due to the switching domains in the film, but an overall or an apparent $P_{fapp}(E_{fapp})$ loop which de facto includes the interface effects at the virgin stage. It is that last loop which will serve as the "reference polarization loop" when the fatigued stage will be addressed further. This new configuration is illustrated in Fig. 4. Under these conditions, the expressions of P_f and E_f above may be simplified and become:

$$P_{fapp} = D - \varepsilon_0 \cdot \varepsilon_{fapp} \cdot E, \quad (7)$$

and

$$E_{fapp} = E, \quad (8)$$

where ε_{fapp} represents the overall or apparent permittivity of the fresh capacitor including the dielectric properties of the interfaces. This value is unknown but can be estimated with a fit method already outlined [26,27]. It was indeed shown in Refs. [26] and [27] that incorrect evaluation of ε_{fapp} yields a rotational shift of the polarization loop computed from relations (7) and (8). The good value of ε_{fapp} is obtained when the $P_{fapp}(E_{fapp})$ loop exhibits horizontal saturated branches (see Fig. 5.a)), hence the necessity to saturate the films. We found for the present work $\varepsilon_{fapp} = 230$.

Next, the apparent polarization loop corresponding to the fatigued stage is in turn calculated from the $D(E)$ loop measured after fatigue cycling. But comparison with the reference polarization loop determined at the virgin state needs to take into account the

changes in the properties of the interface induced by fatigue. These variations, materialized by ΔV_{bi} and ΔC_i , can be removed by using the following modified relations:

$$E_{fapp} = \frac{\Delta C_i}{\Delta C_i + C_{fapp}} \left[E - \frac{1}{d} \left(\Delta V_{bi} + \frac{A \cdot P_f}{\Delta C_i} \right) \right], \quad (9)$$

and

$$P_{fapp} = \left[D - \frac{d}{A} \frac{C_{fapp} \cdot \Delta C_i}{(\Delta C_i + C_{fapp})} \left(E - \frac{\Delta V_{bi}}{d} \right) \right] \frac{\Delta C_i + C_{fapp}}{\Delta C_i}, \quad (10)$$

where:

$$C_{fapp} = \frac{\varepsilon_0 \cdot \varepsilon_{fapp} \cdot A}{d}, \quad (11)$$

as directly deduced from Eqs. (4), (5) and (6). In expressions (9) and (10) above, ΔV_{bi} and ΔC_i are the sole unknowns. ΔV_{bi} may be estimated by considering the increase of the coercive fields, ΔE_c^+ and ΔE_c^- (see Fig. 1.b)):

$$\Delta V_{bi}^+ = V_{biaf}^+ - V_{bibf}^+ = \Delta E_c^+ \cdot d, \quad (12)$$

$$\Delta V_{bi}^- = V_{biaf}^- - V_{bibf}^- = \Delta E_c^- \cdot d, \quad (13)$$

where the superscripts "+" and "-" refer to the positive and negative values, respectively. We found $\Delta V_{bi}^+ = 2.6$ V and $\Delta V_{bi}^- = -3$ V. It should be reminded that the definition of V_{bi} and ΔV_{bi} given above is valid only when the loops, close to saturation, exhibit the same D_{max} values as already mentioned.

Once ΔV_{bi} is determined, ΔC_i is then estimated on arbitrarily testing different values until the apparent polarization loop computed from the fatigued stage matches in the best possible way with the reference loop. We found $\Delta C_i = 1.4$ nF, i.e. a value two times larger than that determined without taking into account the interface screening effects (see the second section). The results of numerical calculations are presented in Fig. 5.b). The hysteresis loop measured after setting a capacitor of 1.5 nF (standardized value) in series with a fresh sample (Fig. 6) shows a very satisfying agreement with that displayed by the fatigued sample, but only in terms of the elongation of the loop. The electrical circuit allowing full duplication of the fatigue stage, including an increase of coercive fields, is now presented.

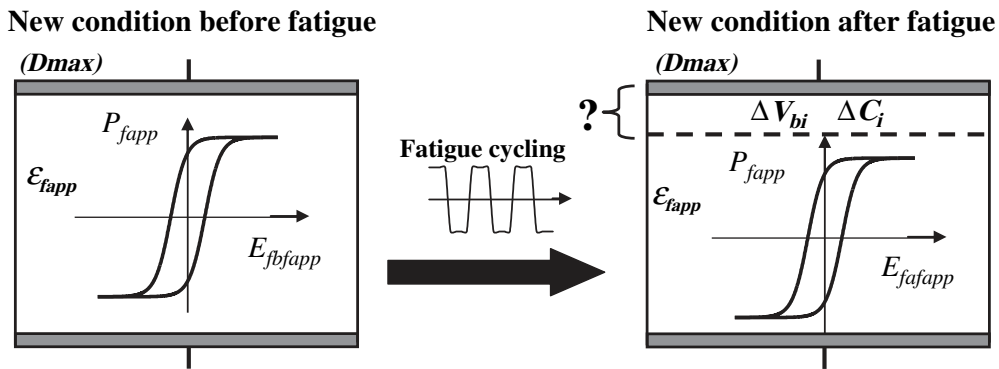


Fig. 4. New configuration where the interface regions at the virgin stage are merged into the bulk layer. The amplitude of the applied voltage, before and after fatigue, is assumed to be set in such way to achieve the same D_{max} value. The apparent polarization loop obtained by this way will serve as a reference loop. If we assume the properties of the bulk layer are not diminished during fatigue cycling, then ΔV_{bi} and ΔC_i become the unknown quantities that can be directly determined by comparing the apparent polarization loop of the fatigued sample to the reference loop.

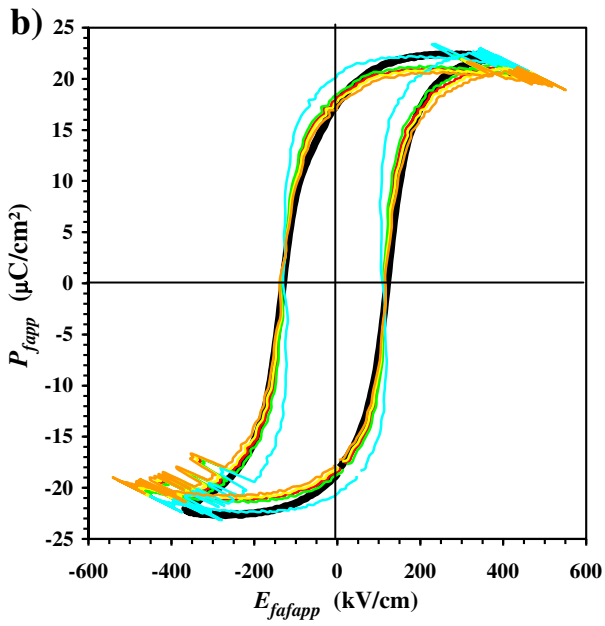
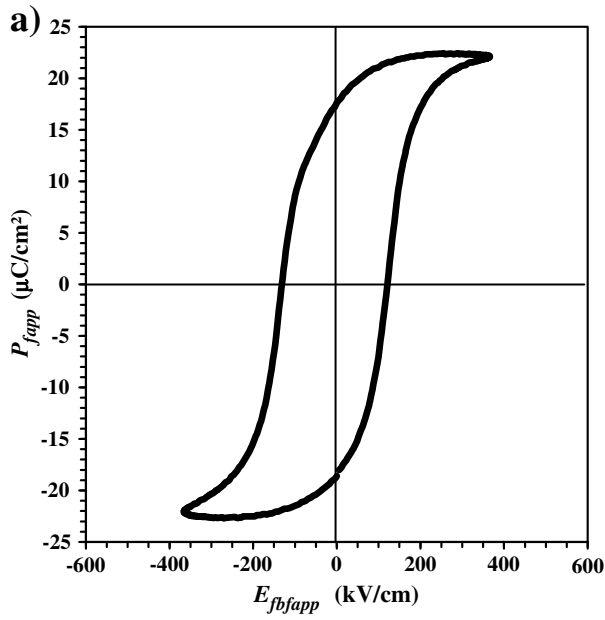


Fig. 5. a) Apparent polarization loop calculated from hysteresis measurement performed on the 400 nm thick PZT capacitor before fatigue (see the plot in thin black line on Fig. 1.a). b) Polarization loop in thick black line is the same plot as a), colored loops are calculated from hysteresis measurement performed after fatigue (loop in thick red line on Fig. 1.b)). Clockwise rotational shift is observed when ΔC_i is over estimated, counter clockwise rotational shift otherwise. The best fit was obtained for $\Delta C_i = 1.4$ nF.

3.2. Full experimental circuit

Fig. 7 depicts the experimental setup we considered for the duplication of the effects of interface charge including the sign switching mentioned above. The results are demonstrated by comparison between Fig. 8.a) and b) and Fig. 1.a) and b) respectively. It must be mentioned that this circuit topology has already been proposed in a previous work to illustrate how the interface charge contributes to increase the coercive values [28]. However at that time the values of the interface capacitances ΔC_{i1} and ΔC_{i2} were set arbitrarily. Moreover, no attempt was made to accurately analyze the sequence of the diode switching.

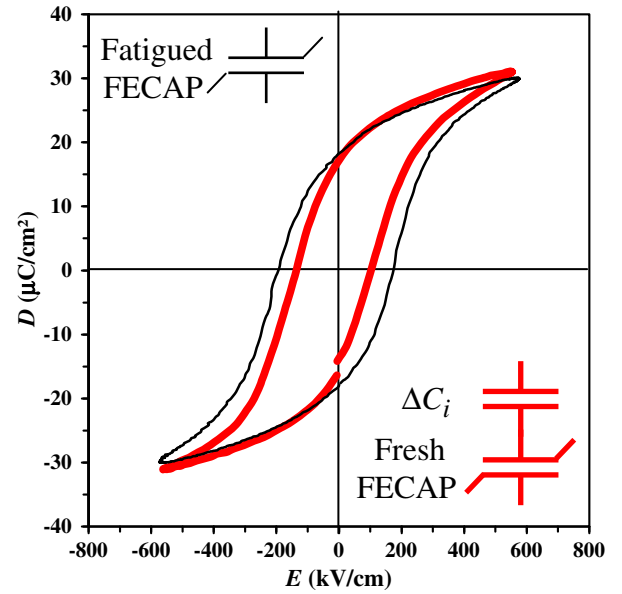


Fig. 6. Hysteresis loops measured on the fatigued PZT capacitor (thin black line) and after connecting a capacitor of 1.5 nF in series with a fresh PZT capacitor (thick red line).

The two capacitors ΔC_{i1} and ΔC_{i2} present the same value of 1.5 nF. They were charged beforehand at 2.6 V and -3 V respectively, according to ΔV_{bi} values found before. The direction of V_{appl} in the figure corresponds to the positive convention used to plot all the hysteresis loops. The circuit was designed so that ΔC_{i1} is put in series with the fresh ferroelectric capacitor at the moment where the voltage V_f across the FECAP reaches its positive coercive value so that the latter increases by ΔV_{bi}^+ . This event occurs when the input voltage V_{appl} reaches its positive coercive value, hence the presence of the diode D1 which then must switch-on, D2 staying switched-off. Conversely, D2 switches-on and D1 switches-off when V_{appl} reaches its negative coercive value at the next half period. ΔC_{i2} is then put in series with the FECAP which negative coercive voltage increases by ΔV_{bi}^- . The final result is shown in Fig. 8.b). The actual fatigue stage (see Fig. 1.b)) is accurately duplicated: increases of coercive and remnant values are recovered, the overall shapes of the hysteresis loops are in good agreement. This is also the case when the voltage is reduced to its initial

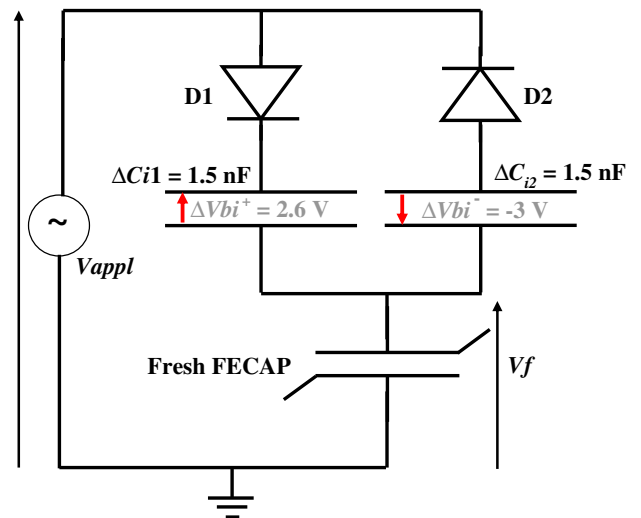


Fig. 7. Enhanced circuit used for the correct duplication of the screening effects caused by accumulation of charge at the interfaces and of the sign switching of this charge.

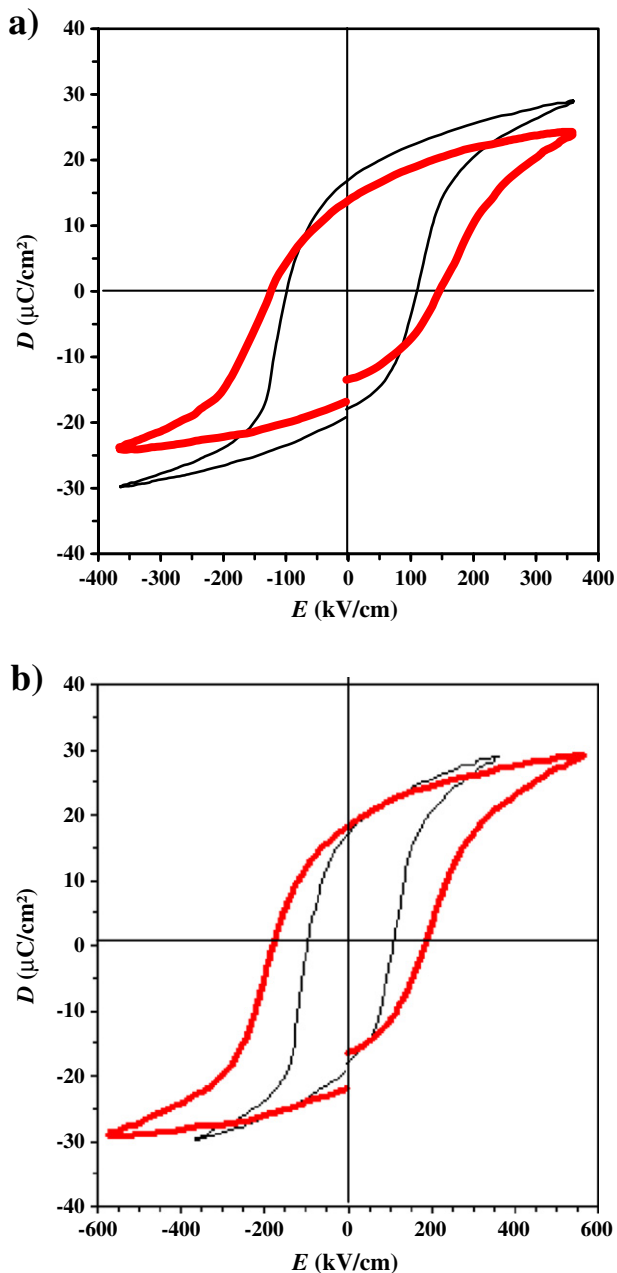


Fig. 8. a) Hysteresis loops of 400 nm thick PZT capacitor before fatigue (thin black line) and after using the circuit in Fig. 7 (thick red line), for same input voltage. b) Same plot as a) except that the voltage applied to the artificially fatigued capacitor was adjusted to achieve the same maximum electric displacement. This artificial fatigue must be compared with actual fatigue presented in Fig. 1.

value, i.e. the value used during fatigue cycling (see Fig. 8.a), to be compared with Fig. 1.a)).

Beyond the unequivocal character of the demonstration, another salient point to be outlined is that the sequence in the sign switching of interface charge assumed above, which was theoretical but is *sine qua non* condition for a realistic simulation of size effect and fatigue [17–20], is here experimentally duplicated. This means that the diodes *actually* switch-on at the moments when $\frac{\partial V_{appl}}{\partial t}$ changes sign, not when V_{appl} changes sign like in most of rectifying circuits, as confirmed by observation of a phase shift of about 90° between the input voltage and the voltage across the diodes. This may be understood

knowing that a diode may indeed be switched-on either by application of a positive voltage across it, or by forcing a current from its anode. Now all the components of the circuit, i.e. the ferroelectric and interface capacitors, are reactive loads in which the current is driven by the derivative of the charge hence of the voltage. Thereby, although the electrical network used represents only a picture of the fatigue mechanism at a given instant, the analysis above strongly suggests that fatigue in PZT films, as well as the size effect, is fundamentally governed by injection of charge from the interfaces. Charge injection occurs when the polarization reverses. At the next polarization reversal, charge is ejected only partly due to trapping defects at the interfaces. So the charge is gradually accumulating, hence a progressive deterioration of the electric properties of the interfaces. The result is a slow decrease of the electric field actually applied to the switching domains, followed by an apparent loss of polarization.

4. Summary

By referring to our previous works which assumed that aging of PZT thin films originates from the deterioration of dielectric and electrostatic properties of the interfaces, we have developed a series electrical network capable of experimentally duplicating the fatigue stage of the ferroelectric capacitor. However the correct evaluation of the series capacitance indispensable for the good duplication of the elongation of the hysteresis loop observed after fatigue cycling required the non-linear character of the switching charge as well as the screening effects of the interface charge to be considered. At the same time, the correct duplication of the increase of coercive and remnant values is possible on condition to utilize charged capacitors with two diodes as driving components.

The fact that hysteresis deformations caused by fatigue cycling were entirely duplicated unequivocally proves the validity of the starting hypothesis: build-up of interface depolarization field, more or less compensated for by interface charge, was the main aging factor. Polarization fatigue is therefore the manifestation of a progressive decline of the electric field actually applied to the switching domains. This mechanism is fundamentally governed by injection of charges from the electrodes, progressively trapped at interface defects.

Our analysis considered the polarization in the sample at two different instants of the fatigue cycling. Further efforts are needed to duplicate the full kinetics of the polarization fatigue.

References

- [1] J. Scott, C.P. de Araujo, *Science* 246 (1989) 1400.
- [2] K. Uchino, in: *Ferroelectric Devices*, Marcel Dekker, New York, 2000, p. 126.
- [3] R. Ramesh, W.K. Chan, B. Wilkens, H. Gilchrist, T. Sands, J.M. Tarascon, V.G. Keramidias, D.K. Fork, J. Lee, A. Safari, *Appl. Phys. Lett.* 61 (1992) 1537.
- [4] C.B. Eom, R.B. Van Dover, J.M. Philips, D.J. Werder, J.H. Marshall, C.H. Chen, R.J. Cava, R.M. Fleming, D.K. Fork, *Appl. Phys. Lett.* 63 (1993) 2570.
- [5] T. Nakamura, Y. Nakao, A. Kamisawa, H. Takasu, *Appl. Phys. Lett.* 65 (1994) 1522.
- [6] J.J. Lee, C.L. Thio, S.B. Desu, *J. Appl. Phys.* 78 (1995) 5073.
- [7] R. Ramesh, H. Gilchrist, T. Sands, V.G. Keramidias, R. Haakenaasen, D.K. Fork, *Appl. Phys. Lett.* 63 (1993) 3592.
- [8] J.F.M. Cillessen, M.W.J. Prins, R.M. Wolf, *J. Appl. Phys.* 81 (1997) 2777.
- [9] M.-S. Chen, T.-B. Wu, J.-M. Wu, *Appl. Phys. Lett.* 68 (1996) 1430.
- [10] A.K. Tagantsev, I. Stolichnov, E.L. Colla, N. Setter, *J. Appl. Phys.* 90 (2001) 1387.
- [11] X.J. Lou, *J. Appl. Phys.* 105 (2009) 024101.
- [12] N. Sama, R. Herdier, D. Jenkins, C. Soyer, D. Remiens, M. Detalle, R. Bouregba, *J. Cryst. Growth* 310 (2008) 3299.
- [13] C.Z. Pawlaczyk, A.K. Tagantsev, K. Brooks, I.M. Reaney, R. Klissurska, N. Setter, *Integr. Ferroelectr.* 8 (1995) 293.
- [14] H.N. Al-Shareef, B.A. Tuttle, W.L. Warren, T.J. Headley, D. Dimos, J.A. Voigt, R.D. Nasby, *J. Appl. Phys.* 79 (1996) 1013.
- [15] E. Paton, M. Brazier, S. Mansour, A. Bement, *Integr. Ferroelectr.* 18 (1997) 29.
- [16] G. Le Rhun, G. Poullain, R. Bouregba, G. Leclerc, *J. Eur. Ceram. Soc.* 25 (2005) 2281.
- [17] R. Bouregba, N. Sama, C. Soyer, G. Poullain, D. Remiens, *J. Appl. Phys.* 107 (2010) 104102.
- [18] G. Poullain, C. Cibert, R. Bouregba, *J. Appl. Phys.* 106 (2009) 124105.
- [19] R. Bouregba, G. Le Rhun, G. Poullain, G. Leclerc, *J. Appl. Phys.* 99 (2006) 034102.
- [20] R. Bouregba, N. Sama, C. Soyer, D. Remiens, *J. Appl. Phys.* 106 (2009) 044101.

- [21] P.K. Larsen, G.J.M. Dormans, D.J. Taylor, P.J. van Veldhoven, *J. Appl. Phys.* 76 (1994) 2405.
- [22] T. Hase, T. Sakuma, Y. Miyasaka, K. Hirata, N. Hosokawa, *Jpn. J. Appl. Phys.* 32 (1993) 4061.
- [23] A.K. Tagantsev, I.A. Stolichnov, *Appl. Phys. Lett.* 74 (1999) 1326.
- [24] A.K. Tagantsev, M. Landivar, E. Colla, N. Setter, *J. Appl. Phys.* 78 (1995) 2623.
- [25] G. Le Rhun, R. Bouregba, G. Poullain, *J. Appl. Phys.* 96 (2004) 5712.
- [26] R. Bouregba, G. Poullain, *Ferroelectrics* 274 (2002) 165.
- [27] R. Bouregba, G. Poullain, *J. Appl. Phys.* 93 (2003) 522.
- [28] G. Le Rhun, Ph.D. thesis, University of Caen, France, 2004, p. 125.